Cold Nuclear Matter Effects on Heavy Flavor Production

R. Vogt

Lawrence Livermore National Laboratory, Livermore, CA 94551, USA
Physics and Astronomy Department, UC Davis, Davis, CA 95616, USA

based on:
RV, arXiv:2101.02858, Phys. Rev. C 103, 035204 (2021)
RV, arXiv:2207.04347, Phys. Rev. C 106, 025201 (2022)
RV, to be submitted

Figure 1: This work was performed under the auspices of the U.S. Department of Energy by Lawrence Livermore National Laboratory under Contract DE-AC52-07NA27344, the LLNL-LDRD Program under Projects 21-LW-034 and 23-LW-036 and the HEFTY Collaboration.

Heavy Flavors are Important Probes of QCD

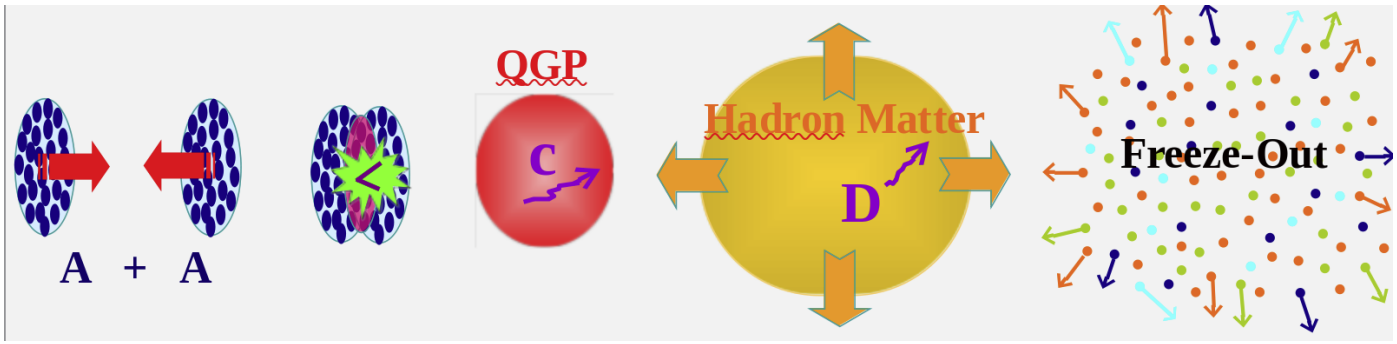

Large mass, $m_Q >> \Lambda_{\rm QCD}$, T, T_c, means heavy quarks produced at early times

Heavy quarks diffuse through the QCD medium and do not thermalize right way, providing a guage of the interaction strength

Allows the study of mass heirarchy in radiative energy loss plus the transition from diffusion to radiation

Hadronization effects probe the medium and study hadron production mechanism, recombination vs. fragmentation through $c \to D$ and $c\bar{c} \to J/\psi$

Many connections to lattice QCD: heavy-quark free energy, heavy flavor fluctuations and correlation functions, dissociation temperature, real and imaginary parts of the quarkonium potential

Study $p+p$, $p+A$ and $A+A$ collisions to differentiate hot and cold matter effects

Many Experimental Programs Study Heavy Flavors

PHENIX and STAR studied open heavy flavor and quarkonium at RHIC, measured nuclear suppression factor R_{AA} and flow v_2 for J/ψ and D mesons up to $\sqrt{s_{NN}} = 200$ GeV, in $p+p$, $p+A$, ($A = \mathrm{He}$, Al, Au, d+Au, Au+Au, U+U

STAR recently separated Υ(1S), Υ(2S) and Υ(3S) states at RHIC; sPHENIX is turning on now and will have better separation of peaks; also plans to study b-jets

LHC experiments have provided a wealth of data on heavy flavor probes, including those at RHIC up to higher p_T as well as heavy flavor jets and $Z + c$-jets; showed hadronization is different for charm baryons and mesons in medium than in vacuum; $p+p$ collisions at $\sqrt{s} = 5.02$, 7, 8 and 13 TeV; $p+\mathrm{Pb}$ at $\sqrt{s_{NN}} = 5.02$ and 8 TeV; Pb+Pb at $\sqrt{s_{NN}} = 2.76$ and 5 TeV

J/ψ and ψ(2S) measurements in ultraperipheral collisions and semi-peripheral collisions probe gluon content of the nucleon and nucleus

LHC experiments also studying exotic hadrons $X(3872)$ and more; LHCb has discovered a plethora of new exotic states, including many potential tetraquark states

LHCb fixed-target studies J/ψ and D mesons at $\sqrt{s_{NN}} = 68.5$, 86.6, and 110.4 GeV in $p + \mathrm{Ne}$, $p + \mathrm{He}$, and $p + \mathrm{Ar}$ collisions respectively; looking for intrinsic charm

Other fixed-target data taken recently or planned: SeaQuest at FNAL, $p_{\mathrm{beam}} = 120$ GeV; COMPASS, NA60+ at CERN SPS, CBM at FAIR; JLab measurement probes gravitational form factor of proton

The EIC will add to heavy-flavor data and theory when it comes on

Intrinsic Charm is a Long-Standing Puzzle in QCD

Intrinsic charm in the proton $|uudc\bar{c}\rangle$, was first proposed in the 1980's

If this state dominates the wavefunction, the charm quarks carry a larger fraction of the hadron momentum, enhancing charm production in the forward x_F region

A number of experimental hints have been seen, no conclusive results

- **Charm structure function, F_2^c, large at largest x and highest Q^2 measured (EMC)**
- **Leading charm asymmetries consistent with intrinsic charm predictions (D^- over D^+ in $\pi^- p$ interactions, E791)**
- **Double J/ψ production observed at high pair x_F by NA3**
- **Forward charm production observed in many fixed-target experiments (WA82, WA89, E791, SELEX and others)**
- **Proposed explanation of high energy astrophysical neutrino rate at Ice Cube (Brodsky and Laha)**
- **LHCb Z+c-jet measurements at forward rapidity consistent with intrinsic charm**

Global PDF analyses have tried incorporating intrinsic charm and reported a range of possible contributions from 0 to 1%, most lately the NNPDF collaboration (Nature)

Model Calculation

Fixed-target experiments can provide evidence of intrinsic charm

The production cross sections are calculated with a combination of perturbative QCD and intrinsic charm contributions; in $p+p$ collisions:

$$\begin{aligned} \sigma_{pp}^{\overline{D}} &= \sigma_{\rm OHF}(pp) + \sigma_{\rm ic}^{\overline{D}}(pp) \\ \sigma_{pp}^{J/\psi} &= \sigma_{\rm CEM}(pp) + \sigma_{\rm ic}^{J/\psi}(pp) \end{aligned}$$

The D meson and J/ψ cross sections are computed at NLO in the color evaporation model for $p+p$ and $p+A$ interactions; $\sigma_{\rm ic}$ is the intrinsic charm cross section

In $p+A$ collisions, nPDF effects, enhanced k_T broadening and nucleon absorption (for J/ψ) included in perturbative QCD cross section:

$$\begin{aligned} \sigma_{pA}^{\overline{D}} &= \sigma_{\rm OHF}(pA) + \sigma_{\rm ic}^{\overline{D}}(pA) \\ \sigma_{pA}^{J/\psi} &= \sigma_{\rm CEM}(pA) + \sigma_{\rm ic}^{J/\psi}(pA) \end{aligned}$$

Heavy Flavor Production in Perturbative QCD

The perturbative QCD cross section at NLO for open heavy flavor and quarkonium is

$$\sigma_{\rm OHF}(pp) \;=\; \sum_{i,j}\int_{4m^2}^{\infty} d\hat{s}\int dx_1\,dx_2\;\; F_i^p(x_1,\mu_F^2,k_{T_1})\;\; F_j^p(x_2,\mu_F^2,k_{T_2})\;\; \hat{\sigma}_{ij}(\hat{s},\mu_F^2,\mu_R^2)\;\;,$$

$$\sigma_{\rm CEM}(pp) \;=\; F_C\sum_{i,j}\int_{4m^2}^{4m_H^2} ds\int dx_1\,dx_2\;\; F_i^p(x_1,\mu_F^2,k_{T_1})\;\; F_j^p(x_2,\mu_F^2,k_{T_2})\;\; \hat{\sigma}_{ij}(\hat{s},\mu_F^2,\mu_R^2)$$

Parton densities factorized into longitudinal (CT10) and a k_T-dependent component to implement k_T broadening a la low p_T resummation; Peterson fragmentation with parameter modified to agree with FONLL included for open charm

$$F^p(x,\mu_F^2,k_T) = f^p(x,\mu_F^2)G_p(k_T)$$

$$G_p(k_T) \;=\; \frac{1}{\pi\langle k_T^2\rangle_p}\exp(-k_T^2/\langle k_T^2\rangle_p)$$

$$\langle k_T^2\rangle_p = \left[1+\frac{1}{n}\ln\left(\frac{\sqrt{s_{NN}}(\mathrm{GeV})}{20\,\mathrm{GeV}}\right)\right]\;\mathrm{GeV}^2$$

$\langle k_T^2\rangle_p$ broadening assumed energy dependent, $n = 12$ from J/ψ data

D Meson $p+p$ Distributions at $\sqrt{s}$ from 68.5 to 110.4 GeV

Uncertainty bands defined by $(m, \mu_F/m_T, \mu_R/m_T) = (1.27 \pm 0.09\,\mathrm{GeV}, 2.1^{+2.55}_{-0.85}, 1.6^{+0.11}_{-0.12})$**;** μ_F**, factorization scale, and** μ_R**, renormalization scale, defined relative to pair transverse mass:** $\mu_{F,R} \propto m_T = \sqrt{m^2 + p_T^2}$ **where** $p_T^2 = 0.5(p_{T_Q}^2 + p_{T_{\overline{Q}}}^2)$

Scale uncertainties set by $\{(\mu_F/m_T, \mu_F/m_T)\} = \{(C,C),\ (H,H),\ (L,L),\ (C,L),\ (L,C),\ (C,H),\ (H,C)\}$ **(Mass uncertainties dominate.)**

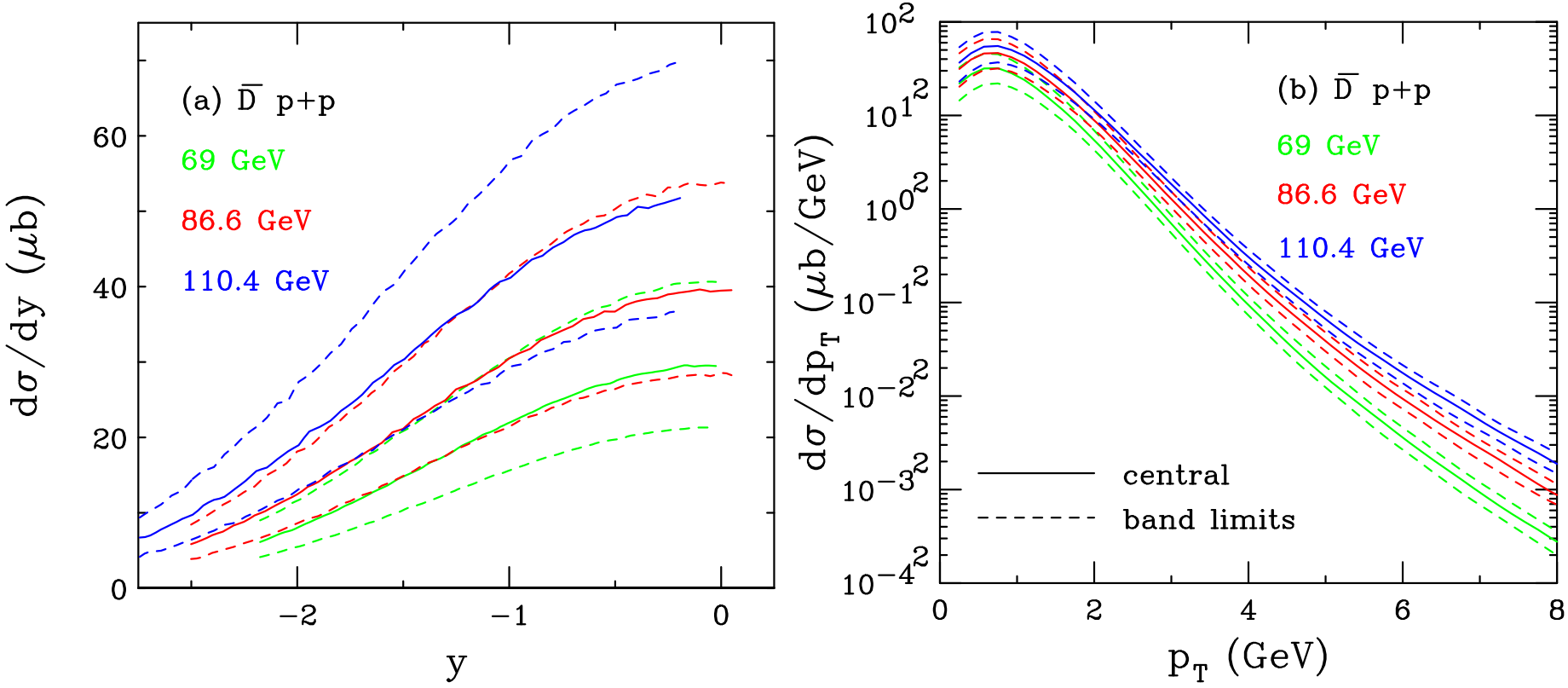

Figure 2: (Color online) The NLO $\overline{D}^0$ production cross sections in $p+p$ collisions at $\sqrt{s}$ = 68.5 (green), 86.6 (red), and 110.4 GeV (blue) as a function of rapidity (a) and p_T (b), in the SMOG fixed-target acceptance, are shown. The solid curves show the central values while the dashed curves outline the upper and lower limits of the uncertainty band.

J/ψ Distributions in $p+p$ at $\sqrt{s}$ from 68.5 to 110.4 GeV

CEM normalization F_C set by comparison to total cross section, same value of F_C is used for all uncertainty sets and all energies

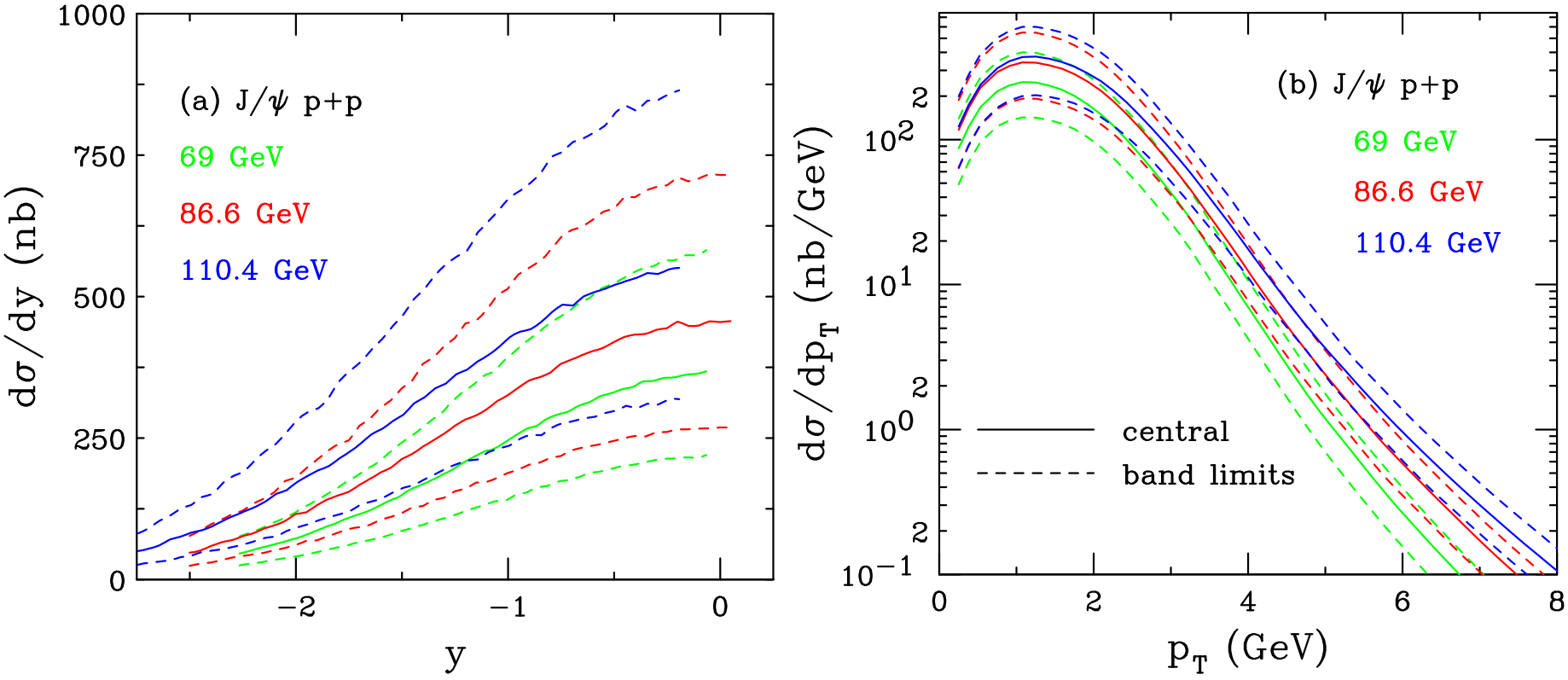

Figure 3: The J/ψ production cross sections in the CEM in $p+p$ collisions at $\sqrt{s} = 68.5$ (green), 86.6 (red), and 110.4 GeV (blue) as a function of rapidity (a) and p_T (b), in the SMOG fixed-target acceptance, is shown. The solid curves show the central values while the dashed curves outline the upper and lower limits of the uncertainty band.

Intrinsic Charm

Probability distribution of five-particle Fock state of the proton:

$$dP_{\mathrm{ic}\,5} = P^0_{\mathrm{ic}\,5} N_5 \int dx_1 \cdots dx_5 \int dk_{x\,1} \cdots dk_{x\,5} \int dk_{y\,1} \cdots dk_{y\,5} \frac{\delta(1-\sum_{i=1}^5 x_i)\delta(\sum_{i=1}^5 k_{x\,i})\delta(\sum_{i=1}^5 k_{y\,i})}{(m_p^2 - \sum_{i=1}^5 (\widehat{m}_i^2/x_i))^2}$$

$i = 1, 2, 3$ are u, u, d light quarks, 4 and 5 are c and $\overline{c}$, N_t normalizes the probability to unity and P^0_{ic} scales the normalized probability to the assumed intrinsic charm content: 0.1%, 0.31% and 1% are used to represent the range of probabilities assumed previously

The IC cross section is determined from soft interaction scale breaking coherence of the Fock state, $\mu^2 = 0.1$ GeV^2

$$\sigma_{\mathrm{ic}}(pp) = P_{\mathrm{ic}\,5} \sigma^{\mathrm{in}}_{pN} \frac{\mu^2}{4\widehat{m}_c^2}$$

The cross sections from intrinsic charm are then obtained by multiplying by the normalization factor for the CEM to the J/ψ while we assume direct correspondence with IC cross section for $\overline{D}^0$

$$\sigma^{\overline{D}}_{\mathrm{ic}}(pp) = F_C \sigma_{\mathrm{ic}}(pp) \quad , \sigma^{J/\psi}_{\mathrm{ic}}(pp) = F_C \sigma_{\mathrm{ic}}(pp)$$

The A dependence is the same for both $\overline{D}$ and J/ψ

$$\sigma_{\mathrm{ic}}(pA) = \sigma_{\mathrm{ic}}(pp)\, A^\beta$$

where $\beta = 0.71$ for a proton beam on a nuclear target, as determined by NA3

Intrinsic Charm Boosted at Forward Rapidity

As $\sqrt{s_{NN}}$ increases, the intrinsic charm rapidity distribution is moved further away from midrapidity, at collider energies it is inaccessible to most forward detectors

The p_T distributions are shown with the rapidity range is restricted to $0 < y < 1$, green curve shows integration over all y; if y acceptance at higher y, more of the IC p_T distribution is captured

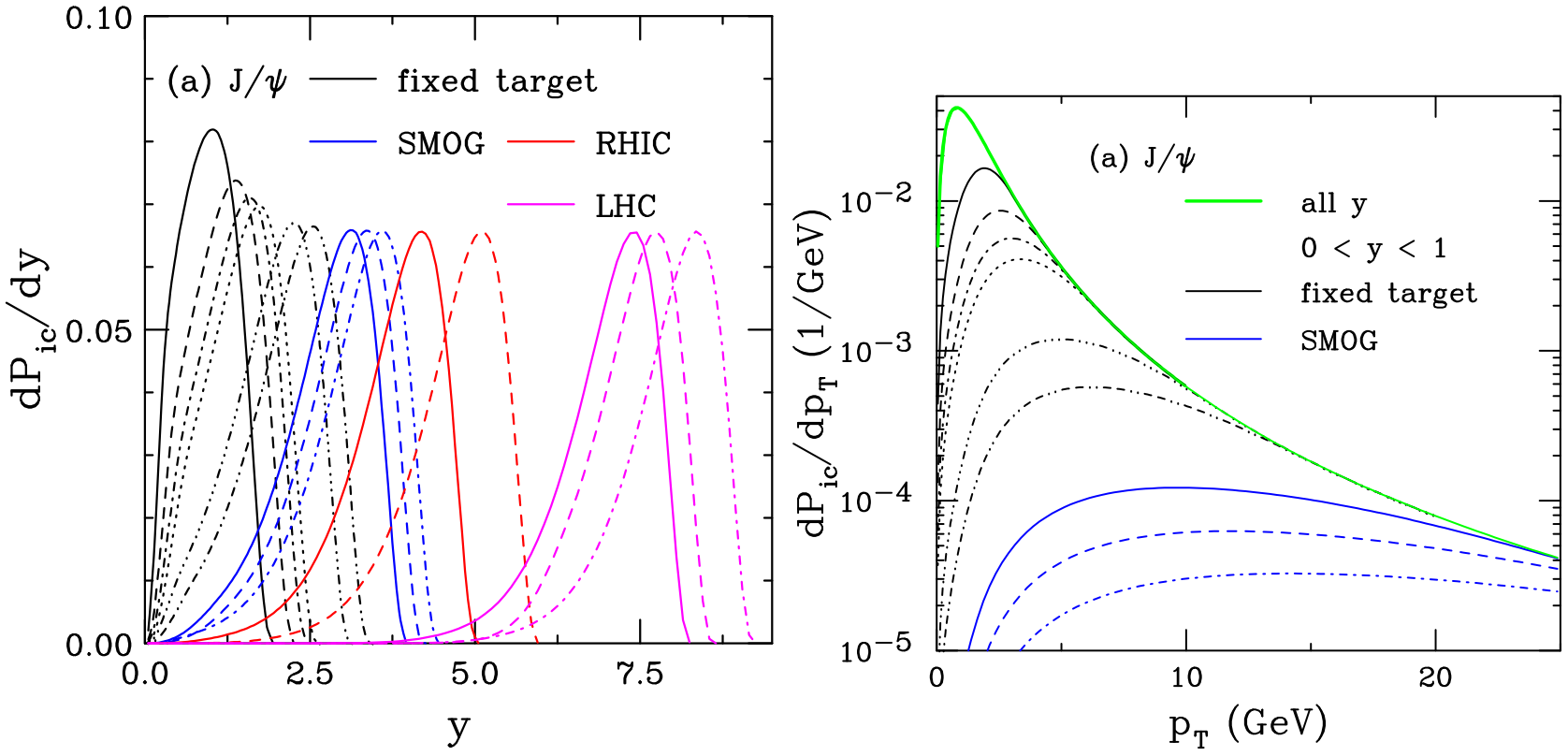

Figure 4: The probability distributions for J/ψ production from a five-particle proton Fock state as a function of y (left) and p_T (right). The rapidity distributions are shown for $\sqrt{s} = 8.8$ GeV to 13 TeV. (Right) The results are shown for all rapidity in the solid green curve. Results for restricting the rapidity range to $0 < y < 1$ are shown for $p_{\rm lab} = 40$, 80 and 120 GeV by the solid black, dashed blue and dot-dashed red respectively.

Summary of Previous Fixed-Target J/ψ Data

NA60 $p_{\rm lab} = 158$ **and 400 GeV, covering** $0.05 < x_F < 0.4$ **and** $-0.075 < x_F < 0.125$ **respectively, were taken on Be, Al, Cu, In, W, Pb, and U targets (PLB 706, 263 (2012))**

NA3 $p_{\rm lab} = 200$ **GeV,** $x_F > 0$**, taken on a Pt target (Z. Phys. C 20, 101 (1983))**

NA50 $p_{\rm lab} = 450$ **GeV, midrapidity** $(-0.1 < x_F < 0.1)$**, used Be, Al, Cu, Ag, W and Pb targets (EPJ C 33, 31 (2004))**

E866 $p_{\rm lab} = 800$ **GeV,** $-0.09 < x_F < 0.95$**, used Be, Fe, and W targets (PRL 84, 3256 (2000))**

HERA-B $p_{\rm lab} = 920$ **GeV,** $-0.34 < x_F < 0.14$**, used C, Ti and W targets (EPJ C 60, 525 (2009))**

Comparison with α Extracted from E866 J/ψ $p+A$ Data

E866 obained α as a function of x_F and p_T (in 3 x_F bins) for $A =$ Be, Fe, and W

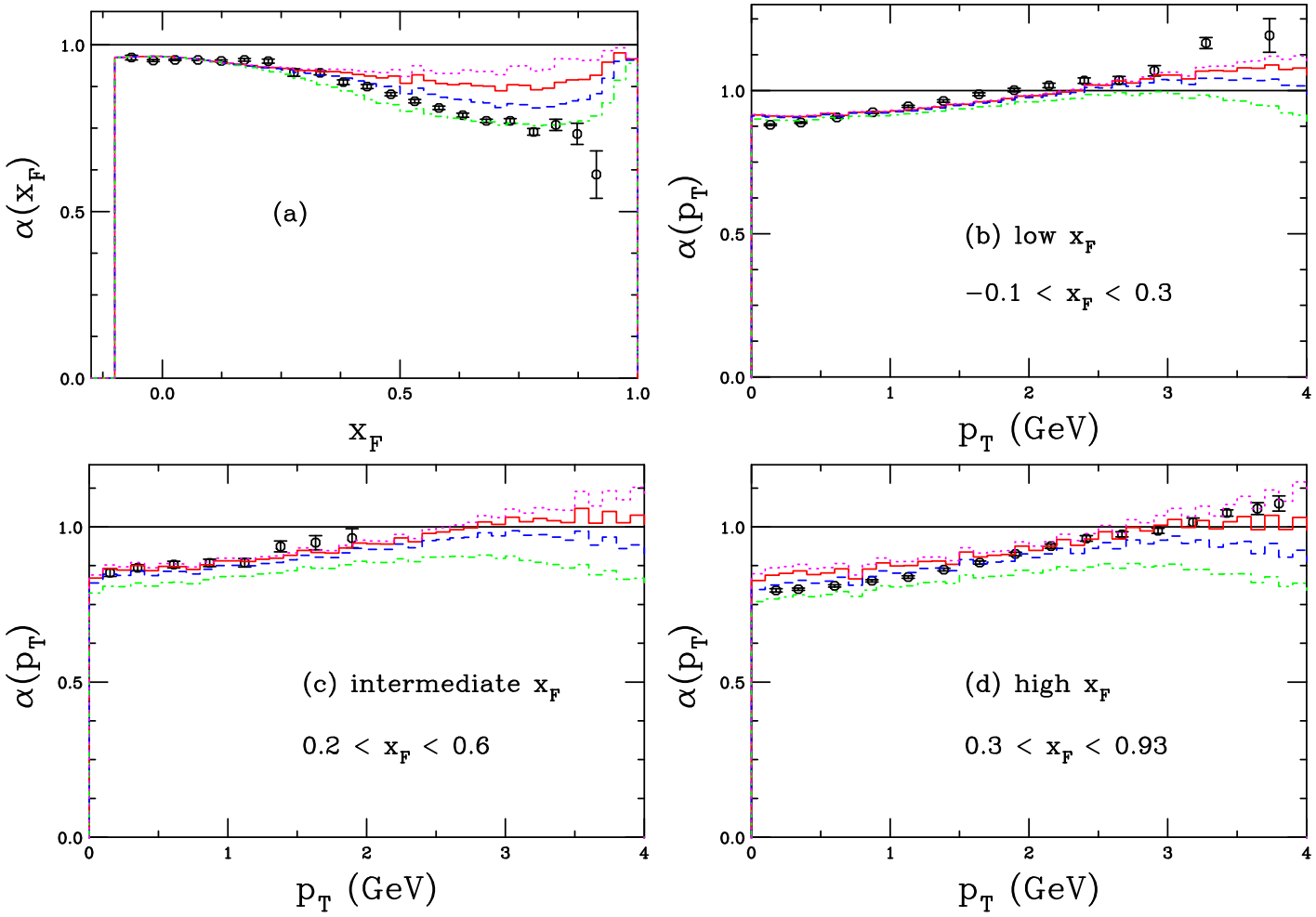

Figure 5: The exponent $\alpha(x_F)$ (a) and $\alpha(p_T)$ for low x_F (b), intermediate x_F (c), and high x_F (d). The dotted magenda curves use $P^0_{\mathrm{ic}\,5} = 0$ while the solid red, dashed blue, and dot-dashed green curves show $P^0_{\mathrm{ic}\,5} = 0.1\%$, 0.31% and 1% respectively. The E866 data (PRL **84**, 3256 (2000)) are the black points. From: RV, PRC **103**, 035204 (2021).

Comparison of $\alpha(x_F)$ with Fixed-Target J/ψ Data

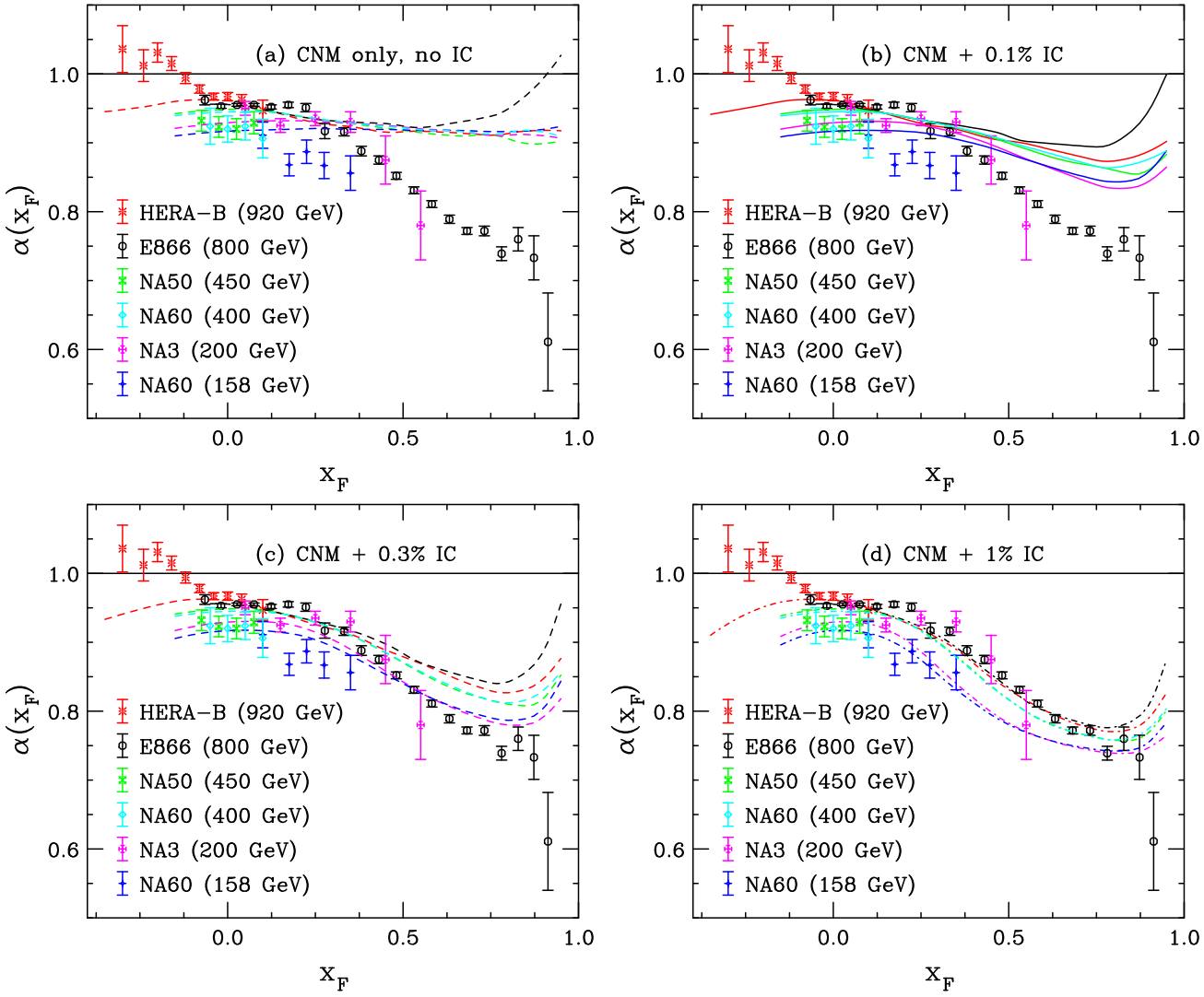

Figure 6: The value of $\alpha(x_F)$ for J/ψ production at: NA60 ($p_{\rm lab} = 158$ GeV), NA3 ($p_{\rm lab} = 200$ GeV), NA60 ($p_{\rm lab} = 400$ GeV), NA50 ($p_{\rm lab} = 450$ GeV), E866 ($p_{\rm lab} = 800$ GeV), and HERA-B ($p_{\rm lab} = 920$ GeV). The points and curves of the same color are at the same energy. Calculations with $P^0_{\rm ic\,5} = 0$ are in (a) while $P^0_{\rm ic\,5} = 0.1\%$, 0.3%, and 1% are shown in (b)-(d).

SMOG $\overline{D}^0$ Results Compared to Calculations

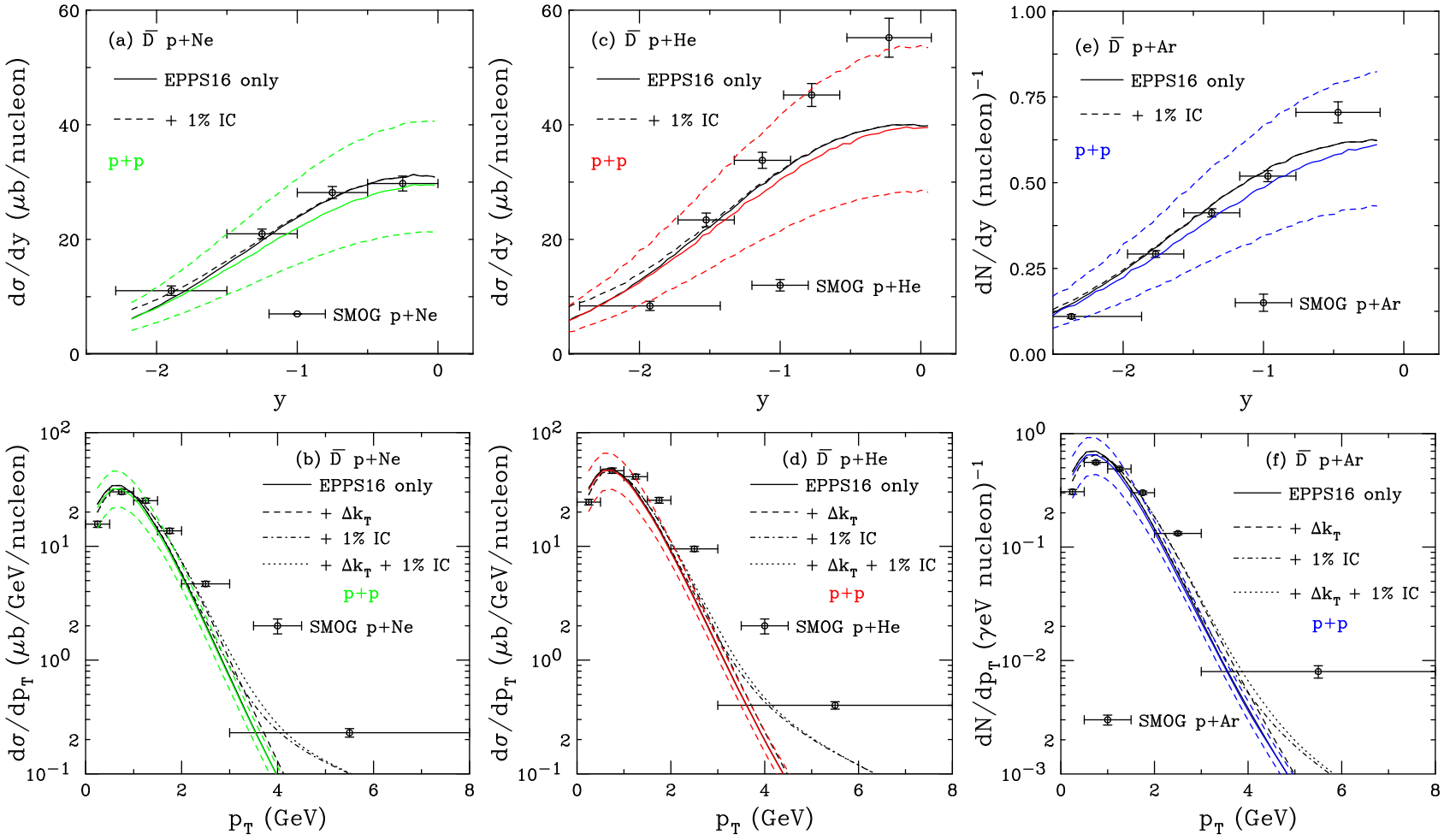

Figure 7: The $\overline{D}$ cross section as a function of y in (a), (c), (e) and p_T in (b), (d), (f) for $p+$Ne ($\sqrt{s_{NN}} = 68.5$ GeV) in (a) and (b); $p+$He ($\sqrt{s_{NN}} = 86.6$ GeV) in (c) and (d); and $p+$Ar ($\sqrt{s_{NN}} = 110.4$ GeV) in (e) and (f). The black curves are the $p+A$ calculations. The colored curves (solid and dashed) show the QCD $p+p$ calculations (no IC). The $p+A$ rapidity distributions are shown for EPPS16 only (solid) and EPPS16 with $P^0_{\rm ic\,5} = 1\%$ (dashed). The p_T distributions show EPPS16 only (solid); EPPS16 with k_T kick (dashed); EPPS16 and $P^0_{\rm ic\,5} = 1\%$ (dot-dashed); and EPPS16, k_T kick and $P^0_{\rm ic\,5} = 1\%$ (dotted). The $p+$Ne data are from arXiv:2211.11633; the $p+$He and $p+$Ar data are from PRL **122**, 132002 (2019).

SMOG J/ψ Results Compared to Calculations

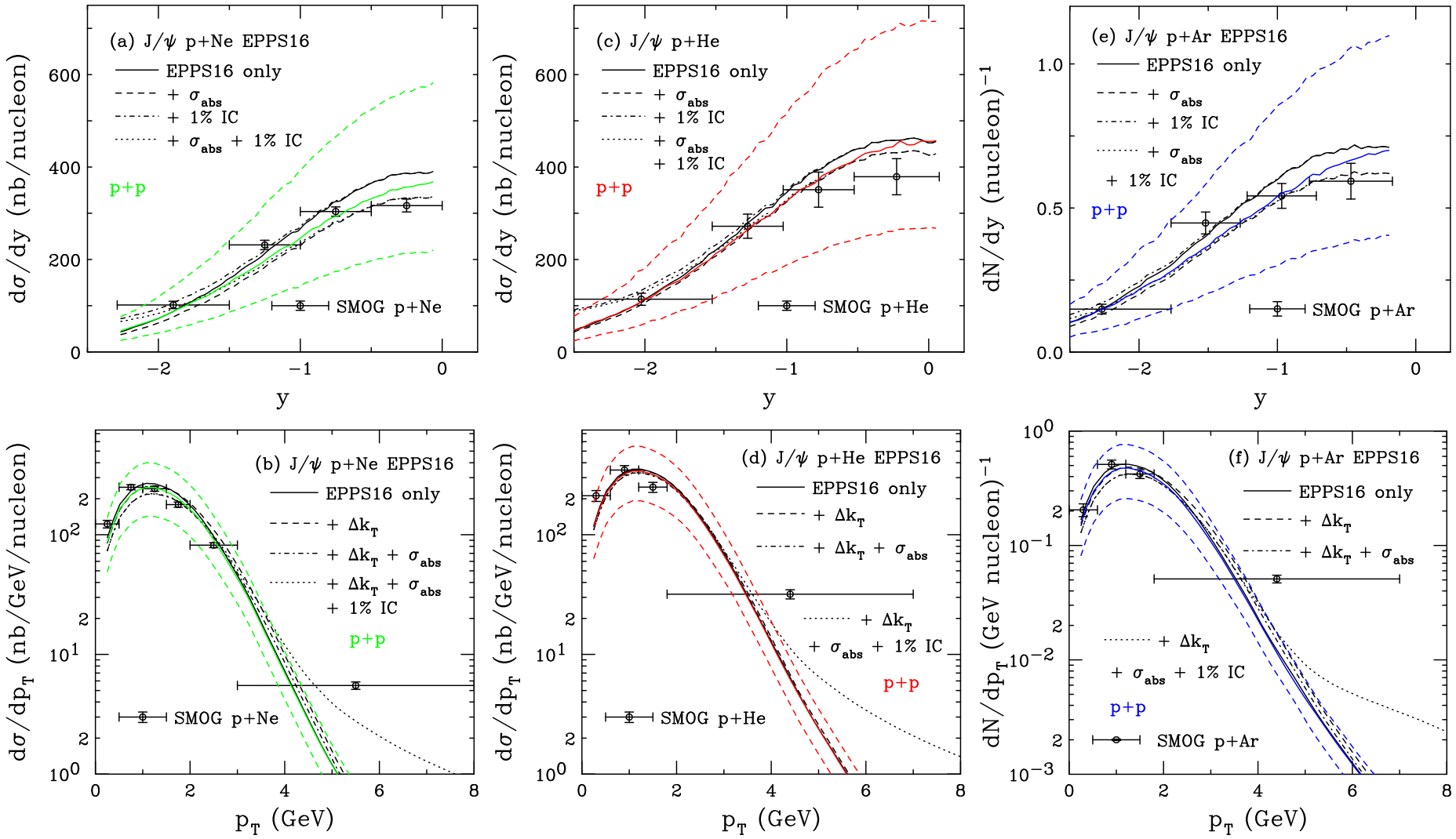

Figure 8: The J/ψ cross section as a function of y in (a), (c), (e) and p_T in (b), (d), (f) for $p+$Ne ($\sqrt{s_{NN}} = 68.5$ GeV) in (a) and (b); $p+$He ($\sqrt{s_{NN}} = 86.6$ GeV) in (c) and (d); and $p+$Ar ($\sqrt{s_{NN}} = 110.4$ GeV) in (e) and (f). The black curves are the $p+A$ calculations. The colored curves (solid and dashed) show the CEM $p+p$ calculations (no IC). The $p+A$ rapidity distributions are shown for EPPS16 only (solid); EPPS16 with absorption (dashed); EPPS16 and $P^0_{\rm ic\,5} = 1\%$ (dot-dashed); and EPPS16, absorption, and $P^0_{\rm ic\,5} = 1\%$ (dotted). The p_T distributions show EPPS16 only (solid); EPPS16 with k_T kick (dashed); EPPS16, absorption, and k_T kick (dot-dashed); and EPPS16, absorption, k_T kick and $P^0_{\rm ic\,5} = 1\%$ (dotted). The $p+$Ne data are from arXiv:2211.11645; the $p+$He and $p+$Ar data are from PRL **122**, 132002 (2019).

J/ψ $p + \mathrm{Pb}$ distributions as a function of y and p_T

Here the p_T distribution is taken in the range $0 < |y| < 1$ for $p_{\mathrm{lab}} = 40$ and 800 GeV and $1.1 < |y| < 2.2$ for $\sqrt{s_{NN}} = 200$ GeV

An enhanced k_T broadening is assumed for $p + \mathrm{Pb}$ collisions

The A dependence of intrinsic charm suppresses its contribution in the lead nucleus

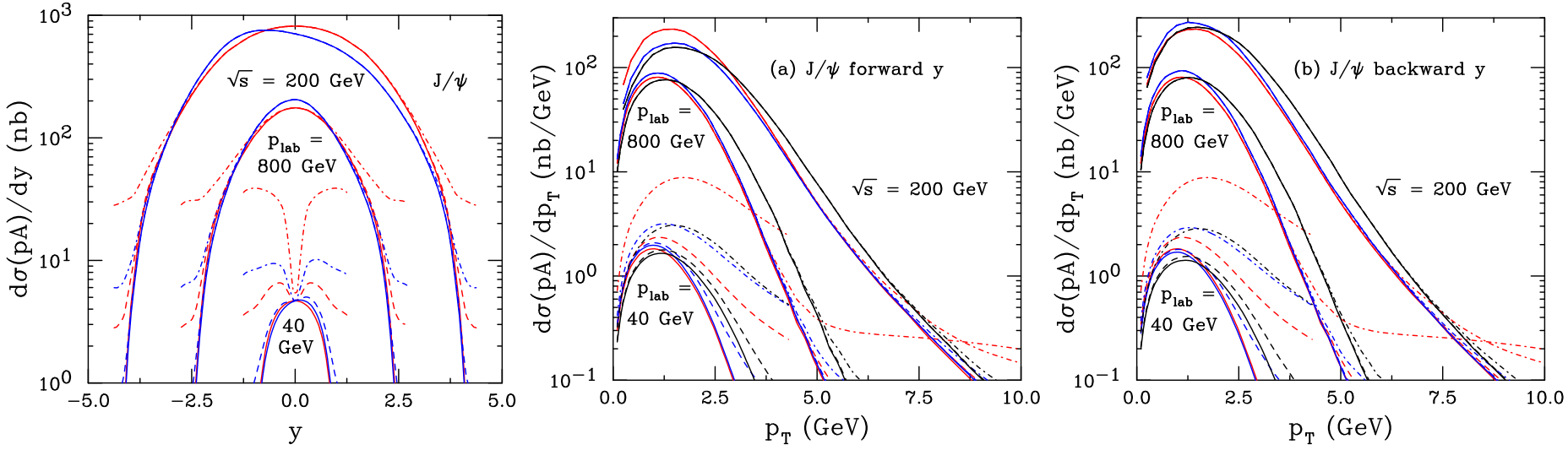

Figure 9: The J/ψ distributions at $p + p$ and $p + \mathrm{Pb}$ (per nucleon) at $p_{\mathrm{lab}} = 40$ and 800 GeV and $\sqrt{s} = 200$ GeV as a function of rapidity (left) and forward (middle, a) and backward (right, b) rapidity. The red curves show the results for $p + p$ collisions while the blue and black curves show the $p + \mathrm{Pb}$ distributions without and with an enhanced intrinsic k_T kick respectively. (The rapidity distributions are independent of the kick.) Three curves are shown in each case: no intrinsic charm (pQCD only, solid); $P^0_{\mathrm{ic}\,5} = 0.1\%$ (dashed); and $P^0_{\mathrm{ic}\,5} = 1\%$ (dot-dashed). No J/ψ absorption by nucleons is considered in the $p + \mathrm{Pb}$ calculation.

HEFTY Topical Collaboration Has Been Formed to Study Heavy Flavor Probes

Ralf Rapp (PI), Peter Petreczky and RV (co-spokespersons)

Co-PIs: Steffen Bass, Xin Dong, Tony Frawley, Yen-Jie Lee, Tom Mehen, Swagato Mukherjee, Jian-wei Qiu, Mike Strickland, Ivan Vitev

Four working groups

- **WG1: In-medium properties of heavy flavor hadrons and quarks using lattice QCD, T-matrix approaches and effective field theories (in-medium quarkonium masses and widths; complex potentai at $T > 0$; transport coefficients and charm quark susceptibilities)**
- **WG2: Heavy flavor production in $p + p$, $p + A$, $e + p$, $e + A$ collisions; push the boundaries of heavy flavor theory in small systems, provide baseline cross sections and cold nuclear matter effects for other working groups**
- **WG3: open heavy flavor transport in heavy-ion collisions; develop and deploy framework for heavy quark transport and hadronization in $A+A$ colliisons using latticeQCD based transport coefficients and rigorous statistical analysis**
- **WG4: Quarkontium transport in heavy-ion colliisons; develop and deploy an integrated quantum transport approach for quarkonia in heavy-ion collisions**
- **All working groups interact with each other and depend on each other's resuts to be successful**

Interdependence of HEFTY Working Groups

HEavy Flavor TheorY in QCD Matter